

## Letter

# Noise-like pulses in dispersion-controlled fiber lasers

Andrey K Komarov<sup>1,2,\*</sup> and Sergey M Kobtsev<sup>1</sup><sup>1</sup> Division of Laser Physics and Innovative Technologies, Novosibirsk State University, Pirogova str. 2, 630090 Novosibirsk, Russia<sup>2</sup> Institute of Automation and Electrometry, Russian Academy of Sciences, Acad. Koptuyg Pr. 1, 630090 Novosibirsk, RussiaE-mail: [komarov@iae.nsk.su](mailto:komarov@iae.nsk.su)

Received 4 April 2023

Accepted for publication 20 June 2023

Published 5 July 2023

**Abstract**

Noise-like pulse generation in ring lasers in which the anomalous dispersion of the cavity fiber is partially compensated by using a normal-dispersion fiber has been studied by numerical simulation. Solitons moving in this cavity are periodically subjected to temporal compression in the anomalous-dispersion fiber and expansion in the normal-dispersion fiber. It has been found that in these lasers, stationary solitons become unstable and passive mode locking occurs through the emission of bunched noise-like pulses consisting of chaotically evolving solitons. The results are relevant to the development of noise-like pulse generation and methods for controlling lasing regimes.

Keywords: fiber laser, noise-like pulse, low-coherence radiation

(Some figures may appear in colour only in the online journal)

**1. Introduction**

Fiber lasers are widely used in various fields of science and technology due to their unique characteristics. At the same time, they have significant potential for further development and improvement. An important advantage of lasers of this type is that they exhibit a wide variety of lasing modes. Passively mode-locked fiber lasers can generate both single pulses and various multisoliton structures [1–3].

Multisoliton generation is due to the quantization of the intracavity laser radiation into identical individual solitons [3]. The properties of the generated multisoliton structures are determined by the nature of soliton interaction. Mutual repulsion of solitons in a laser cavity leads to harmonic passive mode locking [4–6] (multi-soliton generation mode in which the distances between all neighboring solitons are the same).

Soliton attraction results in the formation of bound states of solitons [7–14]. In this case, a pair of solitons forms a two-soliton molecule with quantization of the binding energy and distance between the solitons [12, 15]. An analogy has been established [14] between the emerging soliton structures and the different aggregation states of matter (the existence of a soliton gas, a soliton liquid, a soliton glass, and a soliton crystal).

Significant attention has been paid to the study of fiber lasers generating noise-like pulses [16–27]. These lasers are attractive as sources of high-energy pulses with a broad radiation spectrum whose width can exceed that of the spectral gain contour. In addition, the degree of coherence of the radiation consisting of noise-like pulses can be quite low. These lasers have potential for application in optical tomography, optical radars, fiber-optic sensor systems, etc.

The dynamics of noise-like pulse generation seems paradoxical. Although the solitons forming a noise-like pulse are unstable structures that are in constant random motion and

\* Author to whom any correspondence should be addressed.

change, stochastically appearing in and disappearing from the generation, the noise-like pulse retains its integrity as a well-localized object moving in the laser cavity, which shows its high sustainability and stability. This dynamics of noise-like pulses has been found to be quite common in fiber lasers.

The mechanism of formation and stability of noise-like pulses has been studied by numerical simulation [28]. It has been shown that the cubic–quintic nonlinearity of the refractive index of intracavity elements can lead to passive laser mode locking in the noise-like pulse regime. This nonlinearity can be achieved by using the nonlinear polarization rotation technique to produce nonlinear losses leading to passive mode locking [29]. In this case, the parameters of the polarization rotation system should be chosen so as to obtain the required nonlinearity of the refractive index of intracavity elements at which the stationary soliton regime is unstable, and from the set of possible passive laser mode locking regimes, it is the noise-like pulse regime that occurs. However, an easier way to achieve this goal is to subject a complex multisoliton structure to a periodic stimulus that disrupts the ordering of solitons in the nonlinear system and leads to their stochastization and to the occurrence of the noise-like pulse regime. The aim of this work is to study the possibility of using this approach to implement the noise-like pulse regime in the case of passive mode locking of a fiber laser. The periodic effect on the generated pulse is achieved by forming a ring fiber laser cavity consisting of anomalous- and normal-dispersion fibers. During the passage through the anomalous-dispersion fiber, the solitons are compressed, and when passing through the normal-dispersion fiber, they are stretched. Thus, the emerging structure of the laser radiation is subjected to a periodic stimulus.

The article is structured as follows. In section 2, we present the physical model and basic equations used to study the dynamics of noise-like pulse generation. Section 3 is devoted to numerical simulation of the generation of noise-like pulses and a discussion of the results obtained. In section 4, we discuss the conditions for the formation of noise-like pulses in real laser systems. The main conclusions are given in section 5.

## 2. Physical model and generation equations

The fiber laser under study is schematically shown in figure 1. It includes a fiber amplifier (Amplifier), a nonlinear loss fiber (NL) used to form an ultrashort pulse (localize the radiation in a small volume of the laser cavity to increase the radiation intensity), an anomalous-dispersion fiber (An Disp), a normal-dispersion fiber (Norm/An Disp), which was sometimes replaced by an anomalous-dispersion fiber to compare the lasing regimes for fibers with combined dispersion and with only anomalous dispersion for the same laser parameters. Nonlinear losses can be associated with real saturable absorbers [30–32], or with the nonlinear polarization rotation technique [2, 33], or with nonlinear reflective mirrors [34]. Part of the radiation is extracted from the resonator through an out-pour coupler.

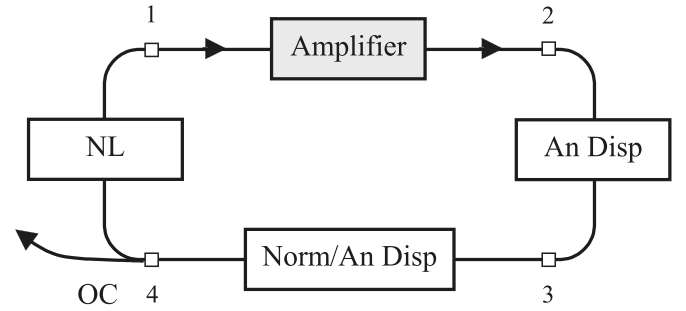


**Figure 1.** Schematic of the investigated laser. (An Disp) is a fiber with anomalous dispersion and a nonlinear refractive index. (Norm Disp) is a fiber with normal dispersion and a nonlinear refractive index. (NL) is a fiber only with nonlinear losses.

To describe the evolution of the field  $E$  in the second (An Disp) and third (Norm/An Disp) fibers, we use the following normalized nonlinear equation [35]:

$$\frac{\partial E}{\partial \zeta} = iD_i \frac{\partial^2 E}{\partial \tau^2} + iqIE, \quad (1)$$

where  $\tau$  is the dimensionless time related to the dimensional time  $t$  as  $t = \tau \delta t$  and the normalized intensity  $I = |E|^2$  is the dimensional intensity  $I'$  in units of  $I_0$  (i.e.  $I' = II_0$ ). The numerical values of the dimensional quantities  $\delta t$  and  $I_0$  are chosen based on the convenience of the numerical simulation. The first term in the equation (1) is related to the dimensionless dispersion  $D_i$  of the fiber refractive index, and the second term is related to its dimensionless nonlinearity  $q$ . The dimensionless dispersion  $D_i$  is given by  $D_i = \beta_2 L_k / (2\delta t^2)$ , where  $\beta_2$  is the dimensional second-order group-velocity dispersion of the fiber medium and  $L_k$  is the length of the corresponding fiber.

It is assumed that the third fiber can have an anomalous dispersion equal to the dispersion in the second fiber  $D_{i2} = D_{i3} > 0$  or a normal dispersion  $D_{i3} < 0$  partially compensating for the anomalous dispersion of the second fiber. The degree of compensation is determined by the length of the normal-dispersion fiber. In this case, a soliton is compressed in passing through the second fiber, and is stretched in passing through the third fiber. Thus, pulses are subjected to a periodic stimulus. If a pulse consists of several solitons, the periodic stimulus leads to their stochastization and the generation of a noise-like pulse.

The dimensionless nonlinearity  $q$  is defined by the expression  $q = \gamma I_0 L_k$ , where  $\gamma$  is the dimensional nonlinearity of the fiber refractive index. For simplicity of analysis, it is assumed that this nonlinearity has the same value  $q_2 = q_3$  for both fibers. The quantity  $\zeta$  is the normalized distance traveled by the field (the sum of the distances traveled, each of which is divided by the quadruple length of the fiber in which this distance was traveled). With this definition of  $\zeta$ , the dimensionless length  $\delta \zeta$  of each of the four fibers is  $1/4$ , and the total dimensionless length of the cavity is 1.

The nonlinear losses  $\sigma_n$  arising in the fourth fiber (NL) are modeled by the following dependence on the intensity  $I$ :

$$\sigma_n = \sigma_1 - pI + p_2 I^2, \quad (2)$$

where the constants  $p > 0$  and  $p_2 > 0$ . At low intensity, the nonlinear losses decrease with increasing intensity. At high intensity, they increase. The nonlinear losses reach a minimum at  $I = I_m$ , where  $I_m = p/2p_2$ . The parameter  $\sigma_1$  is chosen as  $\sigma_1 = p^2/4p_2$ . With this choice, the nonlinear losses remain positive for any intensity and vanish only for  $I = I_m$ . The chosen dependence of nonlinear losses on intensity is qualitatively similar to the corresponding dependence used in the nonlinear polarization rotation technique [36]. The total linear cavity losses  $\sigma$  are determined by the linear losses  $\sigma_1$  and the linear losses due to the radiation output from the cavity  $\sigma_0$  ( $\sigma = \sigma_0 + \sigma_1$ ). For simplicity of analysis, we neglect the dispersion and nonlinearity of the refractive index for the NL and assume that the parameters  $p$  and  $p_2$  are independent of the parameters of the other intracavity fibers.

When the width of the radiation spectrum becomes comparable to the gain bandwidth, field gain analysis requires a more accurate model than the quadratic gain-dispersion model. To analyze the evolution of the field in the first amplifying fiber (Amplifier) of length  $L_1$ , we use a model with a Gaussian gain spectral profile. The change in the field spectral components  $E_\omega$  in the fiber amplifier is described by the equation [37]

$$\frac{\partial E_\omega}{\partial \zeta} = g F_\omega E_\omega, \quad (3)$$

where  $F_\omega$  is the Gaussian spectral gain profile

$$F_\omega = \exp(-D_r \omega^2), \quad (4)$$

and  $g$  is the gain for the central spectral component with  $\omega = 0$ . For the profile (4), the full gain bandwidth  $\Delta\omega_0$  at half maximum  $F_\omega(0)/2$  is given by  $\Delta\omega_0 = 2\sqrt{(\ln 2)/D_r}$ . Taking into account the influence of the spectral contour  $F_\omega$  on the gain saturation leads to the following equation for the gain [38]:

$$g = \frac{a}{1 + (b/2\pi) \int F_\omega |E_\omega|^2 d\omega}. \quad (5)$$

In the case of a narrow-band spectrum ( $F_\omega \approx 1$ ), taking into account the Parseval theorem, from equation (5) we obtain the usual expression for the gain  $g = a / (1 + b \int |E|^2 d\tau)$  [36]. The dispersion and nonlinearity of the refractive index for the amplifying fiber are neglected.

### 3. Numerical simulation results and discussion

In the numerical simulation for the anomalous-dispersion fiber, we used the following values for the physical parameters in the generation equations:  $\gamma = 3 \times 10^{-3} \text{ W}^{-1} \text{ m}^{-1}$ ,  $\beta_2 = 0.015 \text{ ps}^2 \text{ m}^{-1}$ ,  $L_2 = 32 \text{ m}$ ,  $D_r = 0.05$ ,  $D_{i2} = 4$ , and  $q_2 = 8$  (for  $\delta t = 0.24 \text{ ps}$  and  $I_0 = 83 \text{ W}$ ). When using the third normal-dispersion fiber, we set  $D_{i3} = -3.8$  and  $q_3 = q_2$  to partially

compensate for the anomalous dispersion of the second fiber. To confirm the effect on the radiation of the periodic stimulus of fibers with dispersions of opposite signs, we also studied the case where the characteristics of the third fiber coincided with those of the second fiber, i.e.  $D_{i3} = D_{i2}$  and  $q_3 = q_2$  (in this case, the discussed periodic stimulus is absent). For the other parameters of the generation equations, the following values were used:  $a = 1$ ,  $b = 0.2$ ,  $\sigma_0 = 0.05$ ,  $\sigma_1 = 0.2$ ,  $I_m = 2$ ,  $p = 0.2$ , and  $p_2 = 0.05$ . These values were chosen to provide the best fit of the model to real noise-like pulse fiber lasers [14, 39, 40]. The numerical simulation of the evolution of the radiation was performed using the standard split-step fast Fourier algorithm based on the decomposition of the nonlinear dispersive problem into nonlinear and dispersive parts [36, 41].

Figure 2 shows the lasing regime in the case of anomalous dispersion of both fibers ( $D_{i3} = D_{i2}$  and  $q_3 = q_2$ ). In this case for the selected laser parameters, the soliton gas regime [14] occurs after a transient process. The individual solitons shown in figure 2(a) are in constant motion relative to each other due to their different carrier frequencies. Upon collision, they are elastically reflected or pass through each other. The solitons have high mobility so that they do not form bound states (soliton molecules, crystals, and glasses, and information sequences of bound solitons [12]). This is one of the typical generation regimes of passively mode-locked fiber lasers [14]. Figures 2(b) and (c) show the instantaneous radiation spectrum and the spectrum averaged over 2500 passes of the radiation through the cavity. The width of the spectrum is noticeably smaller than the width of the spectral amplification band. It should be noted that for a soliton gas, the spiky single-shot spectrum and the smooth averaged spectrum of solitons in random motion are similar to the spectra for a noise-like pulse (see figures 3(b) and (c)).

The situation changes dramatically when the third fiber is replaced by a normal-dispersion fiber ( $D_{i3} = -3.8$  and  $q_3 = q_2$ , see figure 3). In this case, the noise-like pulse regime is observed. The solitons that form the noise-like pulse (figure 3(a)) are in constant chaotic motion, continuously appearing in and disappearing from the generation. Due to the significant compensation of the anomalous cavity dispersion by the normal-dispersion fiber, the mobility of the solitons associated with their motion relative to each other decreases markedly, and they form a bound state—a stable noise-like pulse. Powerful solitons in the noise-like pulse acquire a significant frequency chirp, leading to a significant spectral broadening beyond the gain spectral bandwidth (see figures 3(b) and (c)). As a result, the efficiency of their amplification decreases, and they lose in competition with weaker solitons with a smaller frequency chirp formed in the pedestal of the noise-like pulse. With increasing intensity, these solitons suffer the same fate as their predecessors, leaving the generation. This also explains the stability of the noise-like pulse: all single solitons outside the noise-like pulse drop out of the generation. Stochastization of solitons is associated with their phase modulation—a nonlinear process that strongly depends

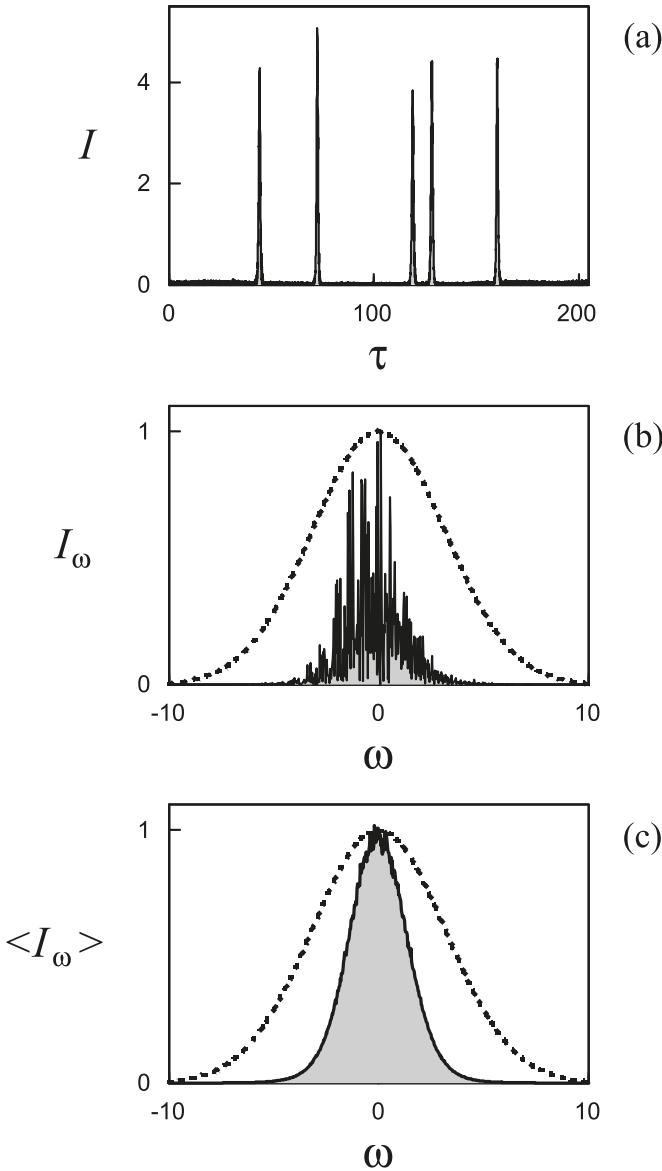


**Figure 2.** Soliton-gas generation regime for  $D_{i3} = D_{i2}$  and  $q_3 = q_2$ . (a) Intensity distribution  $I(\tau)$  and (b) the spectral distribution  $I_\omega$  for  $\zeta = 500$ . (c) Spectral distribution averaged over 2500 passes of the radiation through the cavity. The dashed bell-shaped curve describes the spectral gain profile (see equation (4)).

on the initial characteristics of solitons originated from noise radiation.

To confirm that noise-like pulses are actually due to the presence of alternating-sign dispersion fibers, rather than to a reduction in average anomalous cavity dispersion, we performed the following numerical experiment. We repeated the numerical simulation of the noise-like pulse regime shown in figure 3 changing the fiber dispersion values at  $\zeta = 500$  from  $D_{i2} = 4$  and  $D_{i3} = -3.8$  to  $D_{i2} = D_{i3} = 0.1$ . With this change, the total anomalous cavity dispersion equal to 0.2 was retained, but there was no periodic effect on the radiation associated with the different dispersion values of the fiber segments. As a result, the noise-like pulse regime was transformed into the well-known multi-pulse regime shown in figure 4(a) due to

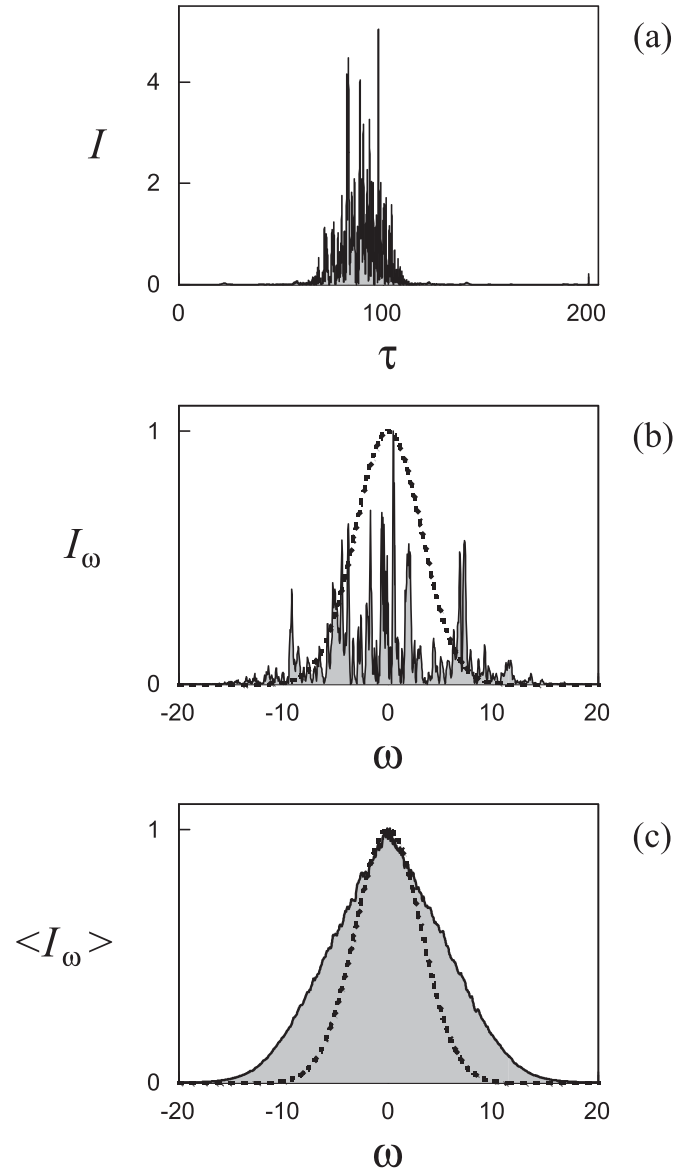


**Figure 3.** Noise-like pulse generation regime for  $D_{i3} = -3.8$ . (a) Intensity distribution  $I(\tau)$  and (b) the spectral distribution of  $I_\omega$  for  $\zeta = 500$ . The dashed curve shows the spectral gain profile. (c) Spectral distribution averaged over 2500 passes of the radiation through the cavity.

the quantization of radiation on individual dissipative solitons [2]. Non-identity of solitons in figure 4(a) is related to their weak interaction through soliton wings. The dependence of the number of these solitons on pumping is the multihysteresis dependence described in [3, 19, 42]. The width of the generated spectrum is approximately the same as that of the spectrum in figure 3. Thus, the presence of fiber segments with alternating-signs dispersion plays a fundamental role in the formation of noise-like pulses.

When  $D_{i2} = 4$  and  $D_{i3} = -3.8$  are replaced by the normal dispersion  $D_{i2} = D_{i3} = -0.5$ , the regime of a single stationary stretched pulse is established after a transient process. With an increase or a decrease in the normal dispersion, the pulse duration increases or decreases, respectively. In the case of

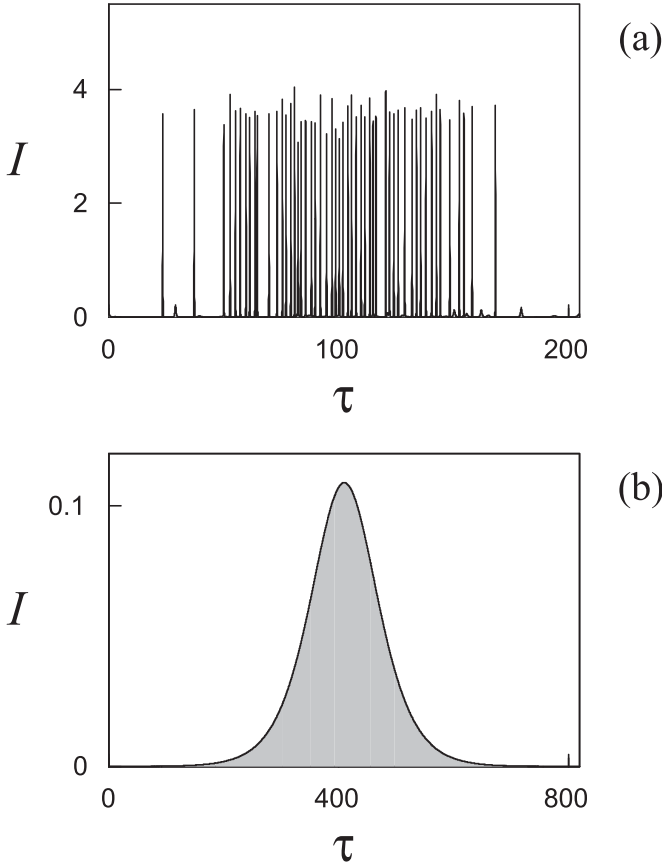


**Figure 4.** (a) Established intensity distribution  $I(\tau)$  for anomalous dispersion  $D_{12} = D_{13} = 0.1$ . The initial distribution  $I(\tau)$  is shown in figure 3(a). (b) Established intensity distribution  $I(\tau)$  for normal dispersion  $D_{12} = D_{13} = -0.5$ .

two cavity fibers with opposite-sign dispersions, when passing through the normal-dispersion fiber, the radiation distribution evolves to the distribution shown in figure 4(a), and when passing through the normal-dispersion fiber, the radiation distribution evolves to the distribution shown in figure 4(b). As a consequence, due to this periodic change in the direction of radiation evolution, the generation regimes shown in figure 4 are not achievable. In this case, a noise-like pulse regime involving mixing of radiations from solitons with different random phases is established after a transient process.

For the noise-like pulse, we also studied the first- and second-order autocorrelation functions of the radiation ( $A_1(\tau_d) = \int E(\tau)E^*(\tau - \tau_d)d\tau$  and  $A_2(\tau_d) = \int I(\tau)I^*(\tau - \tau_d)d\tau$ , respectively). Figure 5 shows the normalized degree of coherence of the pulse radiation  $|\gamma(\tau_d)| = |A_1(\tau_d)|$  [43] and the autocorrelation function  $A_2(\tau_d)$ . The obtained coherence of the noise-like pulse (the height of the pedestal of the function  $|\gamma(\tau_d)|$ ) is only 0.11. That is, the noise-like pulse is low-coherence radiation. The pedestal value for  $A_2(\tau_d)$  is 0.54, which is close to the value (0.50) characteristic for Gaussian noise.

Figures 6 and 7 illustrate the role of the normal-dispersion fiber in radiation stochastization in the simplest case—the single soliton regime at low pump  $a$ . Figure 6 shows the temporal and spectral profiles of a single soliton after a

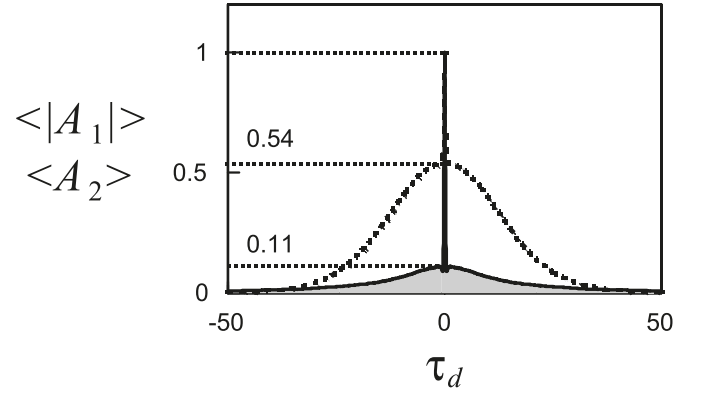


**Figure 5.** Averaged normalized correlation functions of the first order  $|A_1(\tau_d)|$  (solid curve) and second order  $A_2(\tau_d)$  (dashed curve) for the noise-like pulse shown in figure 3. The averaging was carried out over 2500 passes of the radiation through the laser cavity.

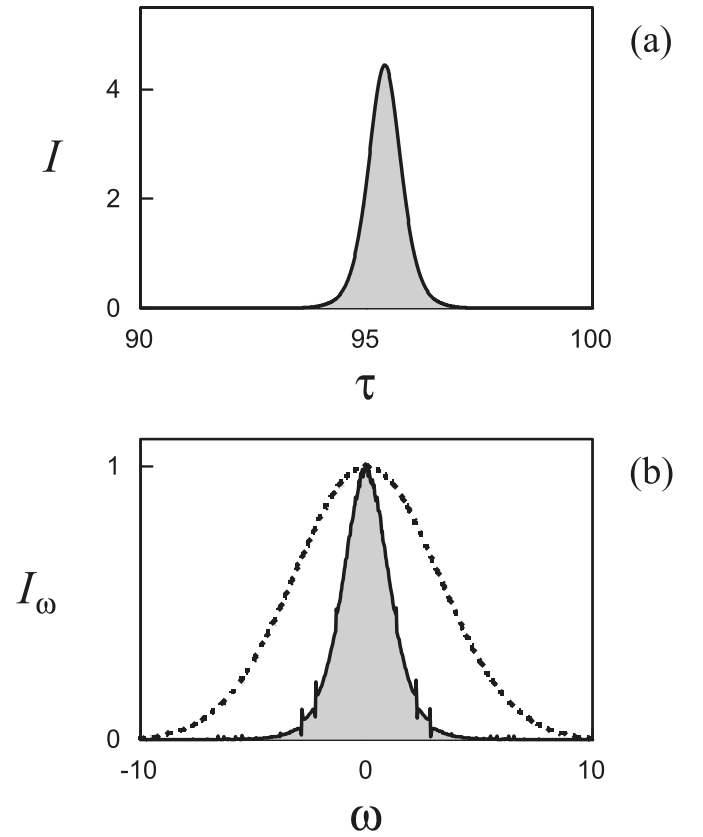


**Figure 6.** Steady-state single-soliton regime for  $D_{i3} = D_{i2}$  and low pump  $a = 0.3$ . (a) Temporal intensity distribution and (b) the spectral distribution for the single soliton.

transient process in the case of the third anomalous-dispersion fiber ( $D_{i3} = D_{i2}$ ,  $q_3 = q_2$ ). In this case, the discussed periodic stimulus due to the difference in fiber dispersion is absent, and the single soliton generation regime with unchanged parameters occurs. In figure 6(b), Kelly peaks are clearly visible in the spectrum. The situation changes dramatically when the third fiber is replaced by a normal-dispersion fiber. In this case, the time and spectral profiles of the soliton change stochastically from pass to pass due to the periodic effect on the soliton

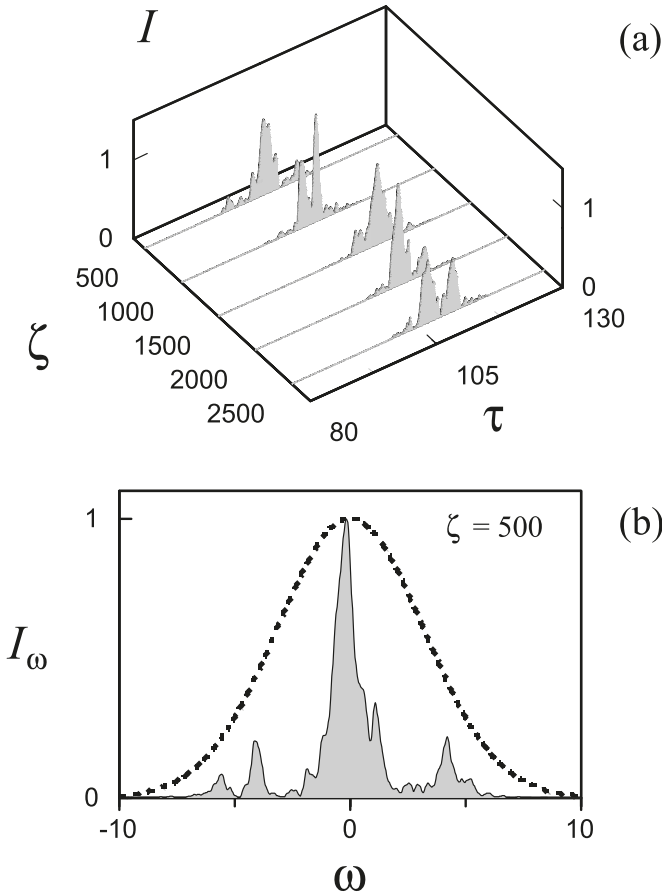


**Figure 7.** (a) Time intensity distribution  $I(\tau)$  as a function of the number of field passes through the cavity  $\zeta$  for the single soliton regime occurring for  $D_{i3} = -3.8$  and low pump  $a = 0.3$ . (b) Instantaneous spectral distribution of the radiation.

caused by the difference in frequency dispersion between the second and third fibers. In this case, the spectrum of the soliton is significantly broadened.

#### 4. On the experimental implementation of the investigated noise-like pulse regime

An erbium fiber laser is a possible candidate for the implementation of the noise-like pulse regime under study. A standard fiber (SMF 28) can be used as the second anomalous-dispersion fiber (see figure 1,  $\beta_2 = 0.015 \text{ ps}^2 \text{ m}^{-1}$ , and  $\gamma = 3 \times 10^{-3} \text{ W}^{-1} \text{ m}^{-1}$ ). It is these parameters of the second fiber that were used in the numerical simulation of the regime under study. The anomalous cavity dispersion due to the second fiber can be partially compensated by using as the third fiber a dispersion-shifted fiber with normal dispersion  $\beta_2 = -0.14 \text{ ps}^2 \text{ m}^{-1}$  [14]. In the numerical simulation, the length of the second anomalous-dispersion fiber was 32 m. To reduce the anomalous cavity dispersion caused by this fiber by a factor of 20, as was done in the above numerical simulation, the third fiber (with normal dispersion) should have a length of 3.26 m.

Passive laser mode locking required to concentrate radiation in a small cavity volume in order to increase its intensity for more efficient phase modulation of radiation due to Kerr nonlinearity can be achieved using the nonlinear polarization rotation technique, as well as real saturable absorbers and nonlinear reflecting mirrors. This creates the conditions for the generation of radiation in the form of individual solitons in an anomalous-dispersion laser cavity.

Of course, in the experimental implementation of the proposed scheme for generating noise-like pulses, it is also necessary to take into account the frequency dispersion of the amplifier and the fiber that creates nonlinear losses. However, a detailed calculation of a specific experimental setup is the next necessary step in the preparation of the experimental implementation of the proposed scheme for generating noise-like pulses.

Note that in [14], partial compensation of the dispersion of an anomalous-dispersion fiber by using a normal-dispersion fiber led to a threefold decrease in the total dispersion of the anomalous cavity. The length of the anomalous-dispersion fiber was 8 m. As a result, along with the soliton gas and soliton crystal regimes, a radiation state similar to a liquid of soliton clusters was obtained in an erbium laser. In this state, the solitons fill only part of the available cavity space and are in motion relative to each other. At the same time, solitons still retain a certain ordered structure at small distances (several soliton lengths). This laser can serve as a prototype for a noise-like pulse laser in which there is no intersoliton structure. An important condition for the efficient generation of noise-like pulses is the closeness of the frequency of the periodic stimulus applied to the radiation due to the passage of the field through fibers with dispersions of opposite signs to the characteristic frequency of relaxation oscillations of solitons that form the generated pulse.

#### 5. Conclusion

In this work, we studied a new method of noise-like pulse generation in passively mode-locked fiber lasers. The proposed mechanism of pulse generation involves the effect of a periodic stimulus on a pulse as it alternatively passes through anomalous- and normal-dispersion cavity fibers: solitons are compressed in the anomalous-dispersion fiber and stretched in the normal-dispersion fiber. The temporal and spectral parameters of the generated noise-like pulses were determined, and first- and second-order auto-correlation functions were calculated. The degree of coherence of the noise-like pulses was found to be low, which opens the way to the development of incoherent lasers based on these pulses. The results help to understand the mechanisms involved in the generation and stabilization of noise-like pulses in fiber lasers. These lasers are attractive for generation of low-coherence noise-like pulses and have significant potential for use in applications that require speckle-free images, in optical tomography, fiber-optic sensor systems, etc.

## Acknowledgments

This paper is sponsored by the Russian Science Foundation and by the Government of the Novosibirsk region under Grant No. 22-12-20010.

## References

- [1] Grudinin A B, Richardson D J and Payne D N 1992 Energy quantisation in figure eight fibre laser *Electron. Lett.* **28** 67
- [2] Tang D Y, Man W S and Tam H Y 1999 Stimulated soliton pulse formation and its mechanism in a passively mode-locked fibre soliton laser *Opt. Commun.* **165** 189
- [3] Komarov A K and Komarov K P 2000 Multistability and hysteresis phenomena in passive mode-locked lasers *Phys. Rev. E* **62** R7607
- [4] Grudinin A B and Gray S 1997 Passive harmonic mode locking in soliton fiber lasers *J. Opt. Soc. Am. B* **14** 144
- [5] Sobon G, Krzempek K, Kaczmarek P, Abramski K M and Nikodem M 2011 10 GHz passive harmonic mode-locking in Er-Yb double-clad fiber laser *Opt. Commun.* **284** 4203
- [6] Zhang Z X, Zhan L, Yang X X, Luo S Y and Xia Y X 2007 Passive harmonically mode-locked erbium-doped fiber laser with scalable repetition rate up to 1.2 GHz *Laser Phys. Lett.* **4** 592
- [7] Malomed B A 1991 Bound solitons in the nonlinear Schrödinger-Ginzburg-Landau equation *Phys. Rev. A* **44** 6954
- [8] Akhmediev N N, Ankiewicz A and Soto-Crespo J-M 1997 Multisoliton solutions of the complex Ginzburg-Landau equation *Phys. Rev. Lett.* **79** 4047
- [9] Grelu P, Belhache F, Gutty F and Soto-Crespo J-M 2002 Phase-locked soliton pairs in a stretched-pulse fiber laser *Opt. Lett.* **27** 966
- [10] Grelu P, Béal J and Soto-Crespo J-M 2003 Soliton pairs in a fiber laser: from anomalous to normal average dispersion regime *Opt. Express* **11** 2238
- [11] Liu X 2010 Hysteresis phenomena and multipulse formation of a dissipative system in a passively mode-locked fiber laser *Phys. Rev. A* **81** 023811
- [12] Komarov A, Komarov K and Sanchez F 2009 Quantization of binding energy of structural solitons in passive mode-locked fiber lasers *Phys. Rev. A* **79** 033807
- [13] Liu X 2011 Interaction and motion of solitons in passively-mode-locked fiber lasers *Phys. Rev. A* **84** 053828
- [14] Amrani F, Haboucha A, Salhi M, Leblond H, Komarov A and Sanchez F 2010 Dissipative solitons compounds in a fiber laser. Analogy with the states of the matter *Appl. Phys. B* **99** 107
- [15] Soto-Crespo J-M, Akhmediev N, Grelu P and Belhache F 2003 Quantized separations of phase-locked soliton pairs in fiber lasers *Opt. Lett.* **28** 1757
- [16] Horowitz M, Barad Y and Silberberg Y 1997 Noiselike pulses with a broadband spectrum generated from an erbium-doped fiber laser *Opt. Lett.* **22** 799
- [17] Kang J U 2000 Broadband quasi-stationary pulses in mode-locked fiber ring laser *Opt. Commun.* **182** 433
- [18] Tang D Y, Zhao L M and Zhao B 2005 Soliton collapse and bunched noise-like pulse generation in a passively mode-locked fiber ring laser *Opt. Express* **13** 2289
- [19] Tang D Y, Zhao L M, Zhao B and Liu A Q 2005 Mechanism of multisoliton formation and soliton energy quantization in passively mode-locked fiber lasers *Phys. Rev. A* **72** 043816
- [20] Zhao L M and Tang D Y 2006 Generation of 15-nJ bunched noise-like pulses with 93-nm bandwidth in an erbium-doped fiber ring laser *Appl. Phys. B* **83** 553
- [21] Zhao L M, Tang D Y, Wu J, Fu X Q and Wen S C 2007 Noise-like pulse in a gain-guided soliton fiber laser *Opt. Express* **15** 2145
- [22] Kobtsev S, Kukarin S, Smirnov S, Turitsyn S and Latkin A 2009 Generation of double-scale femto/pico-second optical lumps in mode-locked fiber lasers *Opt. Express* **17** 20707
- [23] Lecaplain C and Grelu P 2014 Rogue waves among noiselike-pulse laser emission: an experimental investigation *Phys. Rev. A* **90** 013805
- [24] Jeong Y, Vazquez-Zuniga L, Lee S and Kwon Y 2014 On the formation of noise-like pulses in fiber ring cavity configurations *Opt. Fiber Technol.* **20** 575
- [25] Donovan G M 2015 Dynamics and statistics of noise-like pulses in modelocked lasers *Physica D* **309** 1
- [26] Pottiez O, Bracamontes-Rodriguez Y E, Ibarra-Villalon H E, Hernandez-Garcia J C, Bello-Jimenez M, Lauterio-Cruz J P, Garcia-Sanchez E and Kuzin E A 2018 Numerical study of multiple noise-like pulsing in a dispersion-managed figure-eight fibre laser *Laser Phys.* **28** 085108
- [27] Zhang C, Dong J and Meng Y 2023 Study on the spectral characteristics of noise-like pulses in erbium-doped fiber lasers *Optik* **273** 170471
- [28] Komarov A, Komarov K and Zhao L 2019 Multisoliton hybrid generation of fiber lasers with anomalous dispersion *Phys. Rev. A* **100** 033829
- [29] Komarov A, Leblond H and Sanchez F 2005 Quintic complex Ginzburg-Landau model for ring fiber lasers *Phys. Rev. E* **72** 025604(R)
- [30] Zhang H, Tang D, Knize R J, Zhao L, Bao Q and Loh K P 2010 Graphene mode locked, wavelength-tunable, dissipative soliton fiber laser *Appl. Phys. Lett.* **96** 111112
- [31] Komarov A K, Komarov K P and Mitschke F M 2002 Phase-modulation bistability and threshold self-start of laser passive mode locking *Phys. Rev. A* **65** 053803
- [32] Gui L, Xiao X and Yang C 2013 Observation of various bound solitons in a carbon-nanotube-based erbium fiber laser *J. Opt. Soc. Am. B* **30** 158
- [33] Hideur A, Chartier T, Brunel M, Salhi M, Özkul C and Sanchez F 2001 Mode-lock, Q-switch and CW operation of an Yb-doped double-clad fiber ring laser *Opt. Commun.* **198** 141
- [34] Zhao J, Zhou J, Li L, Shen D, Komarov A, Su L, Tang D, Klimczak M and Zhao L 2020 Nonlinear absorbing-loop mirror in a holmium-doped fiber laser *J. Lightwave Technol.* **38** 6069
- [35] Agrawal G P 2013 *Nonlinear Fiber Optics* 5th ed (Academic)
- [36] Komarov A, Leblond H and Sanchez F 2005 Multistability and hysteresis phenomena in passively mode-locked fiber lasers *Phys. Rev. A* **71** 053809
- [37] Komarov A, Komarov K and Zhao L 2020 Broadband ultrashort pulses in passively mode-locked fiber lasers *Opt. Spectrosc.* **128** 493
- [38] Khanin Y I 2012 *Principles of Laser Dynamics* (Newnes)
- [39] Zhao L M, Tang D Y, Cheng T H, Tam H Y and Lu C C 2008 120 nm bandwidth noise-like pulse generation in an erbium-doped fiber laser *Opt. Commun.* **281** 157
- [40] Soto-Crespo J M, Grelu P and Akhmediev N 2011 Dissipative rogue waves: extreme pulses generated by passively mode-locked lasers *Phys. Rev. E* **84** 016604
- [41] Taha T R and Ablowitz M J 1984 Analytical and numerical aspects of certain nonlinear evolution equations. II. Numerical, nonlinear Schrödinger equation *J. Comput. Phys.* **55** 203
- [42] Haboucha A, Komarov A, Leblond H, Salhi M and Sanchez F 2008 Investigation of multiple pulsing and hysteresis phenomena in the erbium-doped double-clad fiber laser *J. Optoelectron. Adv. Mater.* **10** 164
- [43] Born M and Wolf E 1964 *Principles of Optics* 2nd edn (Pergamon)